Time-Domain-Based Modeling of Carrier Transport in Lateral p-i-n Photodiode

Gaku Suzuki, Kohkichi Konno, Dondee Navarro, Norio Sadachika, Yoshio Mizukane, Osamu Matsushima and Mitiko Miura-Mattausch

Graduate School of Advanced Sciences of Matter, Hiroshima University
1-3-1 Kagamiyama, Higashi-Hiroshima, Hiroshima 739-8530 Japan
E-mail: gaku@hiroshima-u.ac.jp

***Abstract* - Carrier transport mechanism in a lateral p-i-n photodiode (PD) has been described analytically in time domain by adopting a coordinate transformation, where carriers are treated to be stationary in the coordinate system. The developed model correctly predicts the measured delayed response of a PD to a 100ps-Gaussian pulse input, which is not observed in models employing stationary and constant electric field approximations. The inherent PD delay predicted by the model is reflected in the output transient characteristics of an inverter circuit with the PD response used as input.**

I. INTRODUCTION

Recently, optoelectronic integrated circuits (OEICs), which incorporates optical devices into conventional VLSI has been investigated with intense vigor (see e.g., [1, 2]). OEICs are expected to achieve faster circuit operation if optical interconnects are employed in place of conventional metal interconnects.

In order to realize OEICs, it is necessary to develop models which can accurately describe the basic characteristics of key optical devices under DC as well as high-frequency switching. Furthermore, these models must be easily incorporated with existing circuit simulators.

One key device ever developed is the p-i-n photodiode (PD) used as a photodectector in optical interconnects. This device transforms optical signals to electrical ones. There are two factors in characterizing photodiodes. One is the light penetration depth, which depends on the wavelength of incident light pulse. Another is the distance from where the carriers are generated to the electrode. Each factor is associated to an individual direction; light propagation direction and carrier flow direction, respectively.

When both directions coincide, the device is called a vertical p-i-n photodiode (PD), which has been investigated by many authors both numerically [3, 4, 5, 6] and analytically [7, 8, 9]. The cutoff frequency of the vertical type is determined not only by the distance of the carrier flow, but also by light penetration depth. On the other hand, when the two directions are orthogonal, the device is called a lateral p-i-n photodiode [10, 11, 12] as shown in Fig. 1. In such device, the cutoff frequency can become independent of light penetration depth. Thus, even for long wavelength light, high cutoff frequency can be achieved. Compared with the vertical type, only few works have been done so far for the lateral case. Haralson et al.[13] investigated the characteristics of the lateral p-i-n photodiode with a full numerical approach which is not applicable for circuit level simulation. On the other hand, Konno et al. [14, 15] developed an analytical approach for circuit simulation for OEICs. Their approach solved the continuity equation in the frequency domain, and is therefore, compatible with harmonic balance circuit simulation [16].

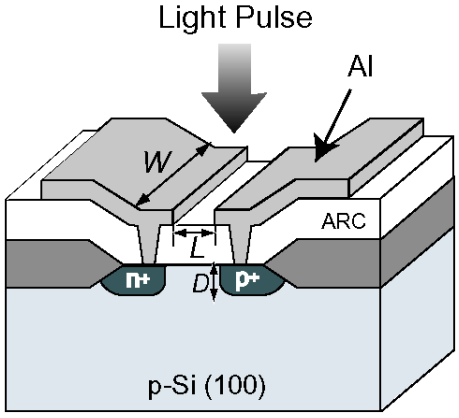

Fig. 1. Typical structure of a lateral p-i-n PD.

In this paper, we obtain a time domain solution for carrier transport in a lateral p-i-n photodiode by using a coordinate transformation. Our model is verified to correctly predict photocurrent response down to ∼100ps pulse. Furthermore, the model is implemented into a time-domain-based circuit simulator and transient response of the device is investigated.

II. FORMULATION OF CARRIER TRANSPORT MODEL IN A LATERAL P-I-N PHOTODIODE

We consider a simplified structure of a p-i-n photodiode shown in Fig. 2 to formulate our model. Here, we assume:

1) homogeneous irradiation only in the intrinsic region,

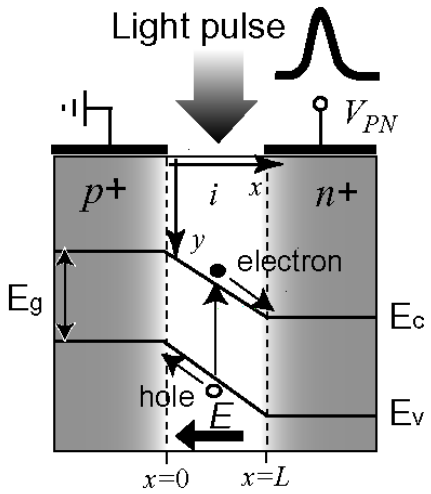

Fig. 2. Simplified structure for developing a model.

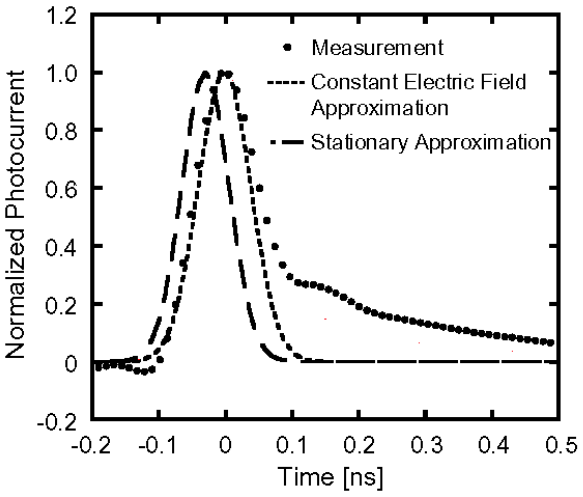

Fig. 3. Comparison between modeling results and measurement. The stationary approximation cannot reproduce the delay. The constant electric field approximation reproduce the general profile but the the end tail cannot be predicted.

2) deep n^+ and p^+ region compared with the light penetration depth,

3) negligible y-component of the electric field $\vec{E} = (E_x, 0)$, where E_x is in general a function of y, in the intrinsic region,

4) negligible change of the electric field due to incident light (see Ref. [17] for high intensity illumination).

The first three assumptions are based on the typical characteristics of a fabricated device designed for high frequency operation. The fourth assumption is justified by the fact that the normal operating condition of the photodiode is in the linear region, in which input optical signal is converted to electric signal without distortion due to the screening effect. Since carriers move along the x direction as shown in Fig. 2, carrier transport equations are simply formulated in one dimension. The equations governing the carrier dynamics are

$$\frac{\partial n(x,y,t)}{\partial t} - \frac{1}{q}\frac{\partial J_{x,n}(x,y,t)}{\partial x} = G_n(y,t), \tag{1}$$

$$\frac{\partial p(x,y,t)}{\partial t} - \frac{1}{q}\frac{\partial J_{x,p}(x,y,t)}{\partial x} = G_p(y,t). \tag{2}$$

Here,

$$J_{x,n} = q\mu_n(E_x)E_x(y)n(x,y,t), \tag{3}$$

$$J_{x,p} = q\mu_p(E_x)E_x(y)p(x,y,t), \tag{4}$$

and

$$G_n(y,t) = G_p(y,t) = \alpha e^{-\alpha y}\phi(t), \tag{5}$$

where n and p are the charge density of electrons and holes respectively, $J_{x,n}$ and $J_{x,p}$ are the current density, $G_{n,p}$ is the carrier generation rate, $\mu_{n,p}$ is the mobility of carriers, α is the absorption coefficient, and ϕ is the photon flux.

We apply the following coordinate transformation to the above differential equations:

$$\xi_{n,p} = \frac{1}{2}\left(t + \frac{x}{v_{n,p}}\right), \tag{6}$$

$$\eta_{n,p} = \frac{1}{2}\left(t - \frac{x}{v_{n,p}}\right), \tag{7}$$

where

$$v_n = -\mu_n E_x, \tag{8}$$

$$v_p = \mu_p E_x. \tag{9}$$

First-order differential equations with respect to ξ, which can easily be solved, are derived. We obtain the final transient photocurrent equation

$$I(t) = \alpha qW \int_0^\infty dy \int_{t-L/|v_p(y)|}^{t} dt' \mu_p(E_x)|E_x(y)|e^{-\alpha y}\phi(t'), \tag{10}$$

where L is the length of intrinsic region, and W is the width of the device. Since the slower carriers, i.e., holes determine the operation speed of the PD, we concentrated on the parameters of hole. If the change of $\phi(t)$ during the time interval $\Delta t \sim L/|v_p|$ is very small, (10) is approximated as

$$I(t) \simeq \alpha qL \int_0^\infty dy e^{-\alpha y}\phi(t) = qL\phi(t), \tag{11}$$

which corresponds to a stationary approximation.

Furthermore, in the case of $|E_x(y)| = E_0 =$ constant down to the light penetration depth, (10) is written as

$$\begin{aligned} I(t) &= q\mu_p E_0 \int_{t-\frac{L}{\mu_p E_0}}^{t} dt'\phi(t'), \\ &\simeq q\mu_p E_0 \sum_i \phi(t_i)\Delta t_i. \end{aligned} \tag{12}$$

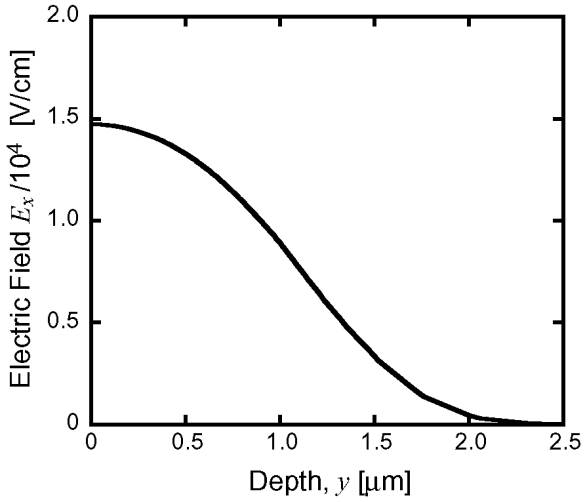

Fig. 4. Simulation result of $E_x(y)$ using 2-dimensional device simulator MEDICI.

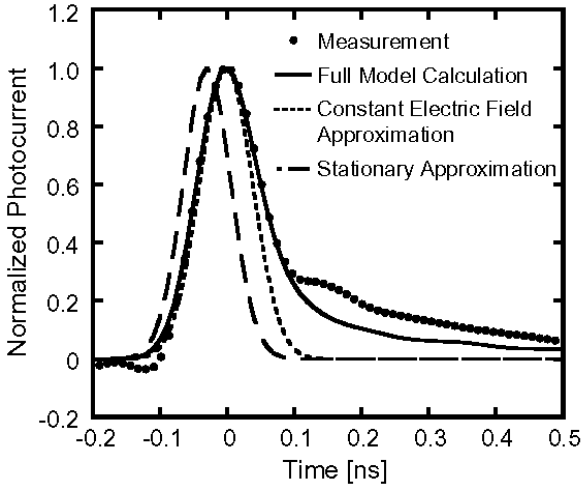

Fig. 5. Comparison between modeling results and measurement. The full model calculation which includes the electric field dependence along the depth direction reproduces the end tail.

In general cases, we have to calculate the expression

$$I(t) \simeq \alpha q \mu_p \left[\sum_i \Delta y_i \left(\sum_j \Delta t_j E_0(y_i) e^{-\alpha y_i} \phi(t_j) \right) \right] \tag{13}$$

numerically. These equations describes the non-stationary features of carrier transport in a lateral p-i-n photodiode.

III. MODELING RESULTS AND DISCUSSION

We have compared the photocurrent calculation results of our model with measurement, which is shown in Fig. 3. For this purpose, we fabricated a silicon lateral p-i-n PD as shown in Fig. 1, where the device dimensions are $L = 2\,\mu$m, $D = 0.5\,\mu$m, and the doping concentration is given by $n^+ \sim 10^{20}\,\mathrm{cm}^{-3}$, $p^+ \sim 10^{20}\,\mathrm{cm}^{-3}$, substrate concentration $\sim 10^{15}\mathrm{cm}^{-3}$. A Gaussian-pulsed laser with wavelength of 532 nm and full-width at half maximum of ~ 100 ps is used as the input light pulse. In this case, the light penetration depth is about 1 μm. The applied bias voltage is $V_{PN} = 2$V. The photocurrent is normalized with respect to the peak value. The stationary approximation shows no delay of the calculated photocurrent. The constant electric field approximation reproduces the general profile of the measured pulse but the end tail can not be predicted. The presence of the tail means that slowly moving carriers exist, which can be found in the deep i-region where the electric field is weak. Simulations with the 2-dimensional device simulator MEDICI [19] reveal that the electric field in the i-region starts from a maximum value at the surface and decays along the depth direction as shown in Fig. 4. To include the y-dependence of the electric field in our model, we assumed the following form of the electric field,

$$E_x(y) = E_0 \exp\left(-\frac{y^2}{d^2}\right), \tag{14}$$

where d characterizes the depth of non-zero electric field and $E_0 \sim V/L$. In our model, the depth d and the mobility μ are model parameters. We adopted $d = 0.5\,\mu$m and $\mu = 350\ \mathrm{cm}^2/\mathrm{V{\cdot}s}$ in this calculation. As seen in Fig. 5, full calculation of (13) taking into account the y-dependence of the electric field describes the tail part more accurately. The remaining difference is considered to be due to the carriers generated in n^+ or p^+ region, which cause slow response because the carrier transport is governed by diffusion.

IV. APPLICATION TO CIRCUIT SIMULATION

In order to investigate the performance of our model, we considered the PD output current as an input to a test circuit in Fig. 6. Simulation is performed in a time-domain-based circuit simulator SPICE. In the test circuit, the PD output current is amplified by an op-amp and converted to a voltage input for an inverter circuit. The PD is implemented by an equivalent circuit shown in Fig. 7, where the independent current source is described by the PD current formulae. Simulation results in Fig. 8 exhibit the inherent longer delay included in the full-model calculation which are not observed in stationary and constant field approximations. The delay is especially visible during the 100ps-rise/fall time of the input signal.

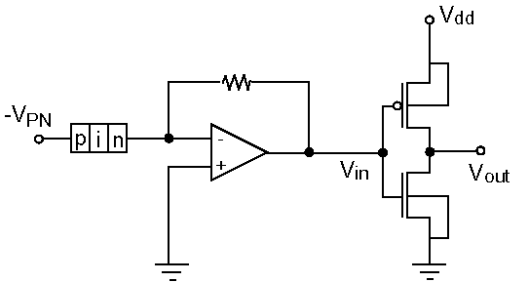

Fig. 6. A transient test circuit. The photodiode response is amplified and converted by an op-amp to a voltage input to an inverter circuit.

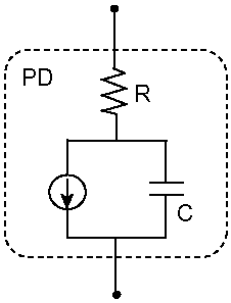

Fig. 7. Implemented equivalent circuit of the photodiode.

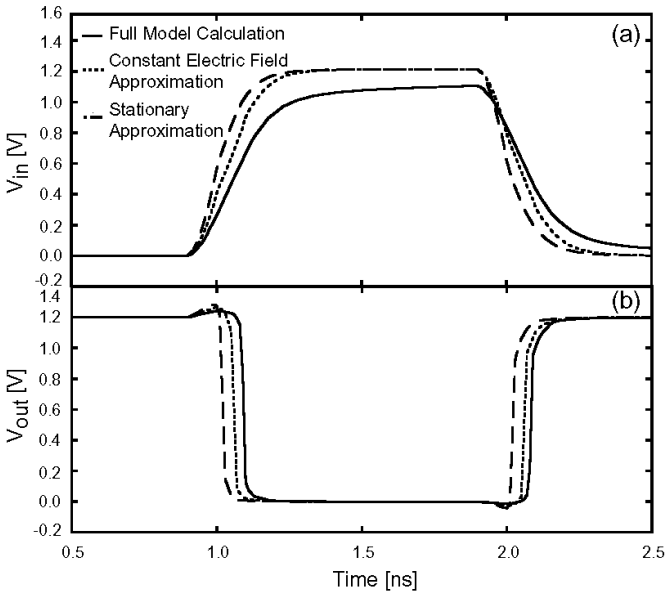

Fig. 8. Output characteristics of the test circuit. (a) Output voltage of the op-amp. The full model calculation shows the inherent delay in PD. (b) Output voltage of the inverter circuit showing the longer delay predicted by the full model calculation.

V. CONCLUSION

We have developed a time-domain description of photoresponse of the lateral p-i-n photodiode, which takes into account the non-stationary features of carrier transport. We also demonstrated the performance of our model using a transient circuit in a circuit-simulator HSPICE. Our model is useful for circuit design of LSI having optical interconnects.

ACKNOWLEDGMENT

This work is supported in part by Research Center for Nanodevices and Systems in Hiroshima University. The authors would like to thank the members of the center for their help in device fabrication and fruitful discussions.

REFERENCES

[1] L. C. Kimerling, Appl. Surf. Sci., **159-160**, p.8 (2000).
[2] J. H. Collet et al., IEEE J. Select. Topics Quantum Electron. **9**, p.425 (2003).
[3] M. Dentan and B. de Cremoux, J. Lightwave Technol., **8**, p.1137 (1990).
[4] J. B. Radunović and D. M. Gvozdić, IEEE Trans. Electron Devices, **40**, p.1238 (1993).
[5] Y. Leblebici et al., J. Lightwave Technol., **13**, p.396 (1995).
[6] P. S. Matavulj et al., J. Lightwave Technol., **15**, p.2270 (1997).
[7] R. Sabella and S. Merli, IEEE J. Quantum Electron., **29**, p.906 (1993).
[8] G. Torrese et al., Microwave and Optical Technology Letters, **31**, p.329 (2001).
[9] K. Konno et al., J. Appl. Phys. **96**, p.3839 (2004).
[10] Y. S. He et al., Electron. Lett., **30**, p.1887 (1994).
[11] M. Ghioni et al., IEEE Trans. Electron Devices, **43**, p.1054 (1996).
[12] M. Yang et al., IEEE Electron Device Lett., **23**, p.395 (2002).
[13] J. N. Haralson II et al., Appl. Phys. Lett., **72**, p.1641 (1998).
[14] K. Konno et al., in Proc. the 2004 International Conference on Solid State Devices and Materials, p.946 (2004).
[15] K. Konno et al., J. J. Appl. Phys., **44**, p.2584 (2005).
[16] K. S. Kundert and A. Sangiovanni-Vincentelli, IEEE Trans. Computer-Aided Design, **5**, p.521 (1986).
[17] O. Matsushima et al., Semicond. Sci. Technol., **19**, p.S185 (2004).
[18] K. Konno et al., Appl. Phys. Lett., **84**, p.1398 (2004).
[19] MEDICI User's Manual, Synopsys, (2003).